Influence of Connection Typology on Seismic Response of MR-Frames with and without "Set-Backs"

Rosario Montuori, Elide Nastri, Vincenzo Piluso, Marina Troisi
Department of Civil Engineering, University of Salerno, Italy

Keywords: semirigid connections, MR-Frames, steel structures, friction devices,

ABSTRACT

The work presented is aimed at the investigation of the influence of beam-to-column connections on the seismic response of MR-Frames, with and without "set-backs", designed according to the Theory of Plastic Mechanism Control (TPMC). The investigated connection typologies are four partial strength connections whose structural details have been designed to obtain the same flexural resistance. The first three joints are designed by means of hierarchy criteria based on the component approach and are characterized by different location of the weakest joint component, leading to different values of joint rotational stiffness and plastic rotation supply and affecting the shape of the hysteresis loops governing the dissipative capacity. The last typology is a beam-to-column connection equipped with friction pads devoted to the dissipation of the earthquake input energy, thus preventing the connection damage. An appropriate modelling is needed to accurately represent both strength and deformation characteristics, especially with reference to partial-strength connections where the dissipation of the earthquake input energy occurs. To this aim, beam-to-column joints are modelled by means of rotational inelastic springs located at the ends of the beams whose moment-rotation curve is characterized by a cyclic behaviour which accounts for stiffness and strength degradation and pinching phenomena. The parameters characterizing the cyclic hysteretic behaviour have been calibrated on the base of experimental results aiming to the best fitting. Successively, the prediction of the structural response of MR-Frames, both regular frames and frames with set-backs, equipped with such connections has been carried out by means of incremental dynamic non-linear analyses.

1 INTRODUCTION

According to the first capacity design principle, the dissipation of the seismic input energy in moment resisting frames has to be concentrated in the so-called dissipative zones, i.e. the end zones of structural members engaged in plastic range, properly detailed in order to assure wide and stable hysteresis loops. In order to design dissipative structures, it is important to promote the plastic engagement of the greatest number of dissipative zones by properly controlling the failure mode. As the plastic engagement of columns can lead to non-dissipative collapse mechanisms, modern seismic codes, such as ANSI-AISC 341-10 [1] and Eurocode 8 [2], suggest the application of the beam-column hierarchy criterion which imposes that, at each beam-to-column joint, the flexural strength of connected columns has to be sufficiently greater than the

flexural strength of the connected beams. However, it is important to underline that the fulfilment of this design criterion is not sufficient to guarantee the formation of a collapse mechanism of global type, but only allows to prevent the development of storey mechanisms [3].

Depending on the beam-to-column joint typology, the dissipative zones can be located at the beam ends or in the connecting elements. In fact, beam-to-column connections can be designed either as full-strength joints, having sufficient overstrength with respect to the connected beam concentrating dissipative zones at the beams ends [4-6], or as partial strength joints, so that the seismic input energy is dissipated by means of the plastic engagement of one or more joint components properly selected.

The use of rigid full-strength joints has been always considered the best way to dissipate the seismic input energy and, therefore, seismic codes provide specific criteria for their design, while there are no detailed recommendations dealing with partial-strength connections.

After some important seismic events, such as Kobe and Northridge, two strategies have been identified to improve the plastic rotation supply of welded connections: the first one consists in the strengthening of the critical area subjected to fracture while the second one promotes the energy dissipation in the beam ends by reducing the bending resistant area of beams in a zone close to beam-to-column connections. This weakening approach is commonly called Reduced Beam Section (RBS) [7-12].

The use of partial-strength joints for dissipating the seismic input energy in the connecting elements of beam-to-column joints has also been introduced in Eurocode 8, being recognised that semi-rigid partial-strength connections, if properly designed by means of an appropriate choice of the joint components where the dissipation has to occur, can lead to dissipation and ductility capacity compatible with the seismic demand.

The use of partial-strength joints, moreover, allows to avoid the plastic engagement of columns without their over-sizing, leading to convenient structural solutions particularly in case of long span MR-Frames [13]. Finally, beam-to-column connections equipped with friction dampers can be considered an innovative type of partial strength connection where the dissipative components are constituted by the damping devices properly located at the beam ends [14-19].

Friction dampers have been proposed in past research activities as passive control devices within the design strategy of supplementary energy dissipation aiming to reduce the damages to the main structural elements, i.e. beams and columns. Passive control devices are typically installed in properly selected locations where high relative displacements occur. In particular, friction dampers present high potential at low cost and are easy to install and maintain, therefore, several friction devices have been experimentally tested and some of these have been used in buildings around the world. In this work friction dampers are not adopted to provide supplementary energy dissipation, but they are rather used to properly substitute the traditional dissipative zones of MR-Frames.

Given the above the main purposes of this paper are, on one end, the evaluation of the influence of beam-to-column connections on the seismic response of MR-Frames, and on the other end, the comparison between the seismic performances irregular MRFs with set-backs) and those of regular MRFs, equipped with the

investigated partial-strength connections. Therefore, the numerical modelling of the cyclic behaviour of partial strength connections is preliminarily presented by properly calibrating the model parameters on the base of available experimental results. Successively, the seismic performances of MR-Frames equipped with such connections are investigated. In particular, for any given structural scheme, the influence of the connection typology is discussed. In addition, for any given connection typology, the influence of the structural scheme, i.e. the influence of set-backs, is examined. To this aim, some study cases are examined by means of incremental dynamic non-linear analyses using SeismoStruct computer program.

2 EXAMINED BEAM-TO-COLUMN CONNECTIONS AND THEIR MODELLING

Semi-rigid steel joints can be designed by means of the component approach [20] codified by Eurocode 3 [21]. This approach allows the prediction of the moment-rotation response of beam-to-column joints provided that the sources of strength and deformability, i.e. all the components, are properly identified. However, Eurocode 3 does not give any indication concerning the modelling of the cyclic behaviour of the joint components, but provides information for evaluating only the monotonic behaviour. For this reason, a significant research activity dealing with the ultimate behaviour of the main components of beam-to-column connections under cyclic actions has been carried out [22-26]. In particular, it has been recently pointed out [27] that the energy dissipation provided by beam-to-column joints under cyclic loads can be obtained as the sum of the energy dissipation due to the single joint components, provided that they are properly identified and their cyclic force-displacement response is properly measured. This result testifies the applicability of the component approach even in the case of cyclic loading conditions. In addition, the actual possibility of extending the component approach to the prediction of the cyclic response of beam-to-column joints has been investigated, leading to the definition of a mechanical model for predicting the cyclic response of bolted connections [28].

Moreover, as the behaviour of bolted beam-to-column connections under cyclic actions can be governed by properly strengthening the components whose yielding has to be prevented [27], the component approach can be also regarded as an effective design tool from the seismic point of view allowing the adoption of hierarchy criteria at the component level, as soon as the dissipative zone, i.e. the weakest joint component, has been properly selected and designed.

The first three beam-to-column typologies herein investigated are partial-strength connections whose structural detail has been designed by means of hierarchy criteria, based on the component approach, aiming to obtain the same flexural resistance, but changing the weakest component. Therefore, they are characterized by different locations of the weakest joint component, leading to different values of the joint rotational stiffness and of the plastic rotation supply [27]. The fourth investigated typology is a beam-to-column connection equipped with friction pads [19, 29-30]. The use of beam-to-column joints equipped with friction dampers allows to obtain MR-Frames where the dissipative zones are constituted by damping devices located at the beam ends.

The reason for investigating these beam-to-column joints is related to the availability of results dealing with their cyclic rotational response, obtained by means of experimental tests performed at the Materials and Structures Laboratory of Salerno University. The structural details of the connections are depicted in Figures 1-4.

In order to point out how the cyclic behaviour is governed by the location of the weakest joint component, the tested specimens have been designed aiming to obtain the same flexural strength, but different values of rotational stiffness and plastic rotation supply. The joint non-dimensional resistance $\overline{m}$, given by the ratio between the joint flexural resistance $M_{j.Rd}$ and the beam plastic moment $M_{b.Rd}$ is equal to 0.76 [27].

Specimen EEP-CYC 02 (Fig. 1) was designed aiming to obtain the aforementioned value of the non-dimensional resistance and relying on the ductility supply of the end-plate, by properly designing its thickness and the bolt location [31]. The first component to be designed is the weakest component, i.e. the end-plate, whose design resistance is obtained as the ratio between the desired joint flexural resistance and the lever arm. Successively, the other components are designed to have sufficient overstrength aiming to avoid their plastic engage.

Specimen EEP-DB-CYC 03 (Fig. 2) is an extended end-plate connection, whose design is aimed at the investigation of the energy dissipation capacity of beams. However, aiming to obtain the same flexural resistance of the previous specimen, RBS (Reduced Beam Section) strategy, called also “dog-bone”, has been adopted. The corresponding structural detail has been designed according to [7].

Specimen TS-CYC 04 (Fig. 3) is a partial-strength joint with a couple of T-stubs bolted to the beam flanges and to the column flanges and designed to be the main source of plastic deformation capacity. The design goal is to avoid the plastic engage of the components related to the column web panel, the column web in compression/tension and the panel zone in shear. The main advantage of double split tee connections is due to their easy repair. In fact, if the panel zone is designed with adequate overstrength, it is possible to substitute only the end T-stubs after a seismic event. Also in this case the same flexural resistance of the other joints was imposed requiring, in addition, a plastic rotation supply of about 0.08 rad [27]. The formulation adopted for predicting the plastic deformation supply of bolted T-stubs are those suggested by Piluso et al. [31].

The last specimen, TS-M2-460-CYC 09, is a bolted double split tee beam-to-column connection equipped with friction dampers designed to slip before the yielding of the beam (Fig. 4) where the energy is dissipated through the slippage between the stem of bolted tee stubs and the beam flange with an interposed friction pad, which are clamped by means of high strength bolts that allow to apply a pre-loading on the surfaces in contact by simply governing the value of the tightening torque and the number and diameter of the bolts. In particular, the structural detail depicted in Fig. 4 has been subjected to experimental tests at the Materials and Structures Laboratory of Salerno University where the influence of different materials adopted as friction pads has been investigated [19, 29-30].

In order to assess the seismic performance of steel moment resisting frames with partial-strength joints, it is preliminarily needed to set up an appropriate model to accurately represent the cyclic rotational behaviour

of connections. In fact, the rotational behaviour of connections under cyclic actions is complicated by the development of strength and stiffness degradation and by pinching phenomena as the number of cycles increases.

As the rules describing these phenomena cannot be deduced by means of theoretical approaches, sufficient experimental data aiming to develop adequately accurate semi-analytical models are needed where the monotonic envelope is predicted by means of the use of mechanical models based on the component method, while the degradation rules are empirically derived by means of the available experimental results [28]. As testified by the developed experimental tests, the cyclic response of connections in terms of shape of the hysteresis loops, stiffness and strength degradation and resulting dissipation capacity are directly related to the components involved in plastic range, mainly the weakest component.

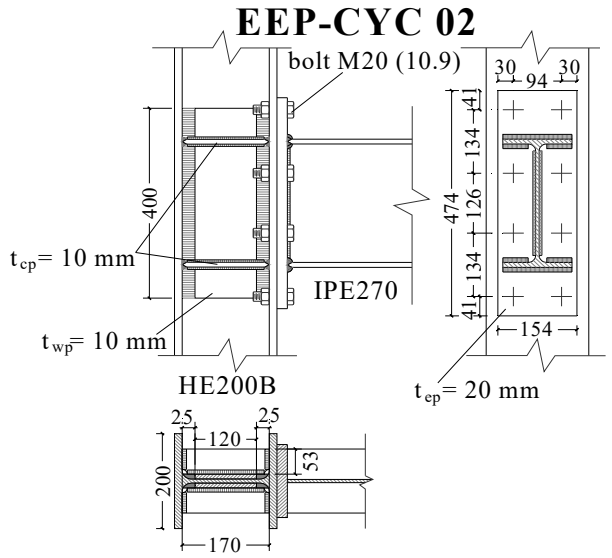

Figure 1. Structural details of EEP-CYC 02 connection

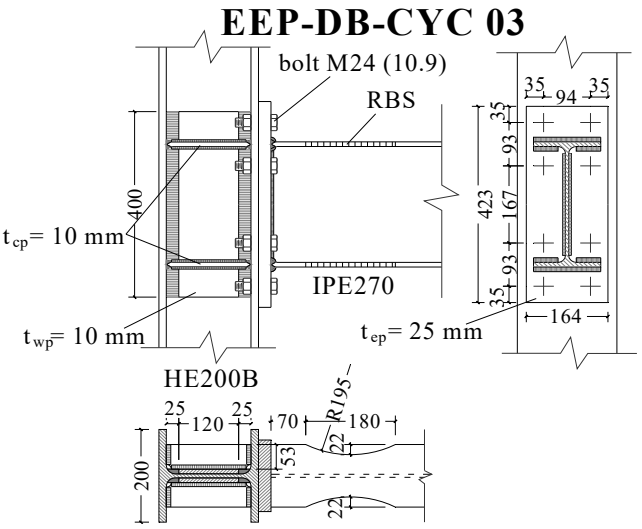

Figure 2. Structural details of EEP-DB-CYC 03 connection

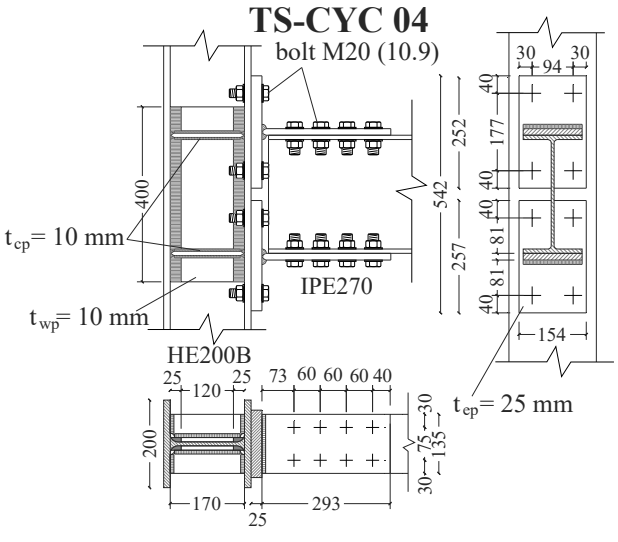

Figure 3. Structural details of TS-CYC 04 connection

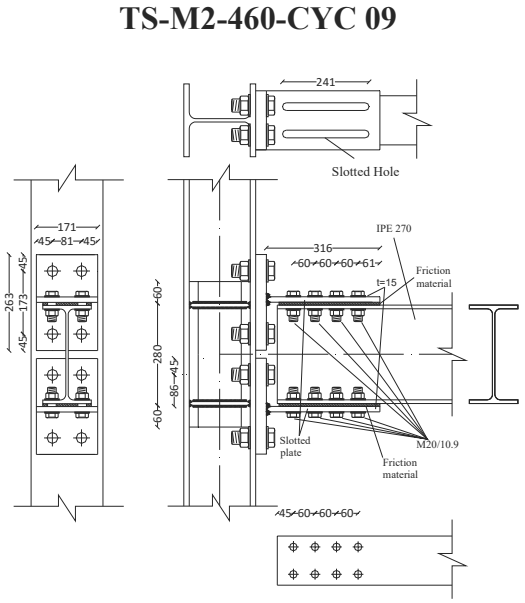

Figure 4. Structural details of TS-M2-460-CYC 09 connection

The non-linear cyclic rotational response of beam-to-column joints has been modelled by means of the spring element included both in IDARC 2D (Version 6.0) and in SeismoStruct (version 3.0) software. The cyclic moment-rotation curve of such spring element has been properly calibrated on the base of available experimental results to account for both stiffness and strength degradation and for pinching phenomenon. In order to derive the parameters governing the cyclic response of the spring elements, a cyclic push-over analysis under displacement control has been carried out with reference to the structural scheme depicted in Fig. 5, having infinitely rigid beam and column elements, whose feature is that its structural response is dependent on the cyclic response of the spring elements only. Therefore, it is possible to apply to such structural model a displacement time-history (where the imposed displacement is equal to the measured joint rotation multiplied by the frame height) exactly reproducing the joint rotation history adopted in testing the beam-to-column joint sub-assemblages and to compare the cyclic moment-rotation response of the spring element with the one obtained from experimental tests. By properly modifying the parameters modelling strength and stiffness degradation and pinching phenomena, it has been possible to select, for each tested specimen, the connection model leading to the best fitting between the analytical model and experimental test results. In particular, the adopted hysteretic model is the Smooth Hysteretic Model (SHM), available in the finite element library of both IDARC 2D and SeismoStruct program, which has also led to a better numerical convergence during the dynamic non-linear analyses with respect to the Polygonal Hysteretic Model (PHM) investigated in previous works [32].

While PHM can be described only by means of few parameters: HC which locates the pivot point, BD and HBE which represent the measure of strength degradation related to ductility and to energy, respectively, the SHM is characterized by additional smoothing parameters which describe the transition from the elastic branch to the plastic branch of the hysteretic cycle. They are: NTRANS which is the parameter governing the elasto-plastic transition (NTRANS=20 corresponds to a bilinear behaviour), ETA which governs the unloading shapes and HSR, HSS, HSM which are the parameters influencing the pinching phenomenon. Finally NGAP, PHIGAP and STIFFGAP take into account the strength increase for high deformation levels. The parameters of the trilinear envelope of the moment-rotation curve of the spring element, adopted in IDARC 2D model and in SeismoStruct model, are delivered in Table 1. In addition, the damage phenomena occurring under cyclic loading conditions have been accounted for by calibrating the corresponding parameters by minimizing the scatter in terms of dissipated energy between experimental test results and numerical results obtained both with IDARC 2D and SeismoStruct spring element.

The comparison between the cyclic moment-rotation curve of the tested connections, depicted in Figures 1 to 4 and the corresponding rotational response, predicted by means of IDARC 2D and SeismoStruct with the spring element modelling parameters given in Table 1 is provided in Figures 6 to 9. From these figures, it can be observed that both IDARC 2D and SeismoStruct provide a satisfactory degree of accuracy in the modelling of beam-to-column joint cyclic behaviour. However, because of the better numerical convergence,

IDA analyses on multi-storey MRFs have been performed by means of SeismoStruct computer program which, in addition, allows a better control of input and output operations, thanks to the graphic interface.

Table 1. Parameters of the spring elements adopted for connection modelling in IDARC 2D and in SeismoStruct

NODO	HC	HBD	HBE	NTRANS	ETA	HSR	HSS	HSM	NGAP	PHIGAP	STIFFGAP
EEP-CYC 02	4	0.05	0.15	1	0.5	0.25	0.03	0.5	8	3	5
EEP-DB-CYC 03	10	0.5	0.01	1	0.5	0.25	10	1	0.2	0.2	0.2
TS-CYC 04	200	0.3	0.35	1	0.5	0.38	0.2	0.45	0.2	0.2	0.2
TS-M2-460-CYC 09	75	0.7	0.4	5	0.5	0.25	100	0.4	2	1000	2

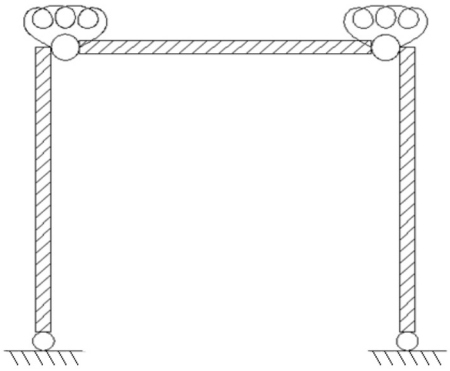

Figure 5. Structural scheme adopted for calibrating spring elements for joint modelling

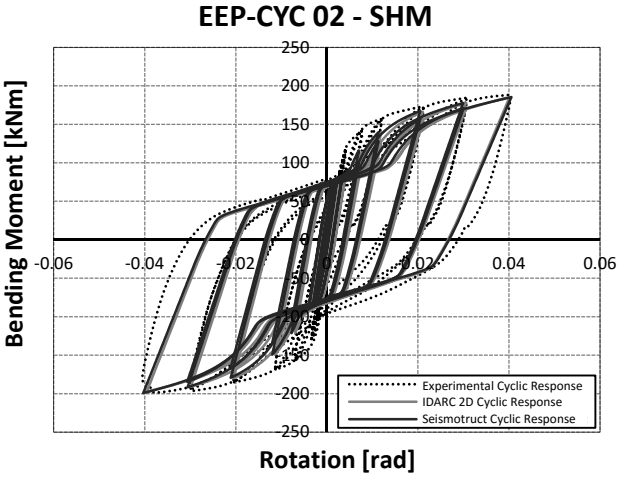

Figure 6. Comparison between the SHM cyclic moment-rotation response of the spring element with the experimental test results for EEP-CYC 02 connection

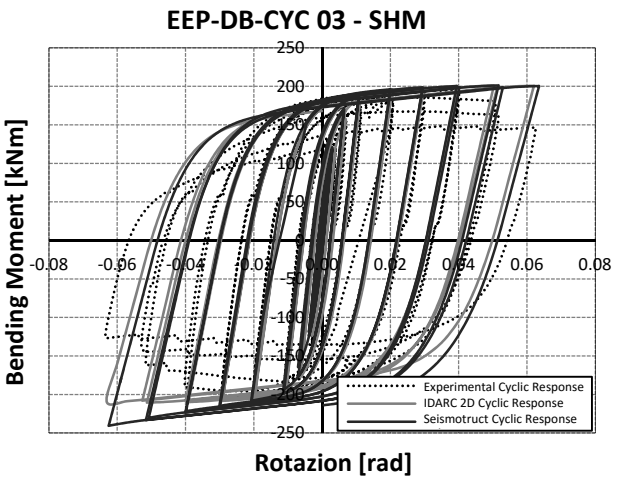

Figure 7. Comparison between the SHM cyclic moment-rotation response of the spring element with the experimental test results for EEP-CYC 03 connection

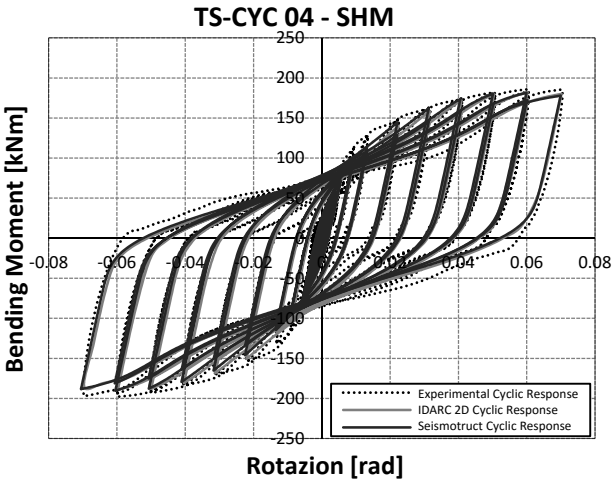

Figure 8. Comparison between the SHM cyclic moment-rotation response of the spring element with the experimental test results for TS-CYC 04 connection

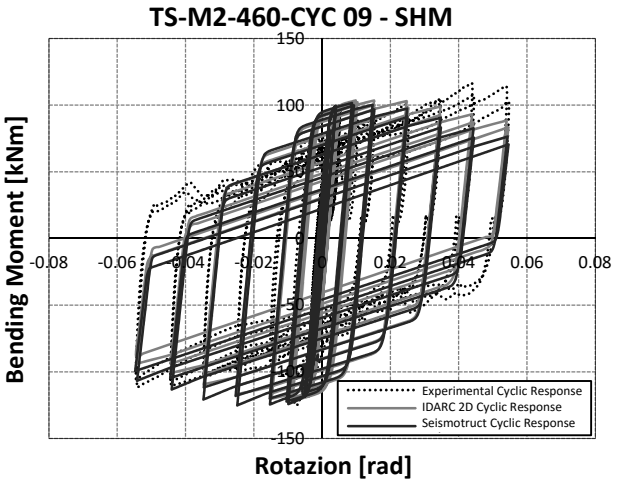

Figure 9. Comparison between the SHM cyclic moment-rotation response of the spring element with the experimental test results for TS-M2-460-CYC 09 connection

3 ANALYSED MR-FRAMES AND THEIR STRUCTURAL MODELLING

The investigated structures (Fig. 10) are a regular MR-Frame with three bays and six storeys and two MR-Frames with "set-backs" constituting irregular frames which result from the regular frame by the introduction of one set-back involving three storeys, namely IRR-1 structure, and four storeys, namely IRR-2 structure, starting from the top. The regular structure was designed accounting for the influence of semirigid connections [33] and imposing a global mechanism [34]. Regarding the design loads, a uniform dead load (G_k) equal to 12.00 kN/m and a uniform live load (Q_k) equal to 6.00 kN/m are applied. The spans of the frames are equal to 6.00 m, while the interstorey heights are equal to 3.20 m with the exception of the first storey whose height is equal to 3.50 m. The uniform vertical load adopted for beam design is $q = 1.35\,G_k + 1.50\,Q_k = 25.2\ kN/m$. A design value of the beam plastic moment approximately equal to $qL^2/8$ has been chosen and IPE270 profiles made of S275 steel grade have been adopted for the beams. The size of the columns of both regular and irregular structures are selected by adopting a rigorous design procedure assuring a collapse mechanism of global type [34-35]. The whole design procedure has been carried out with reference to S275 steel grade. However, in order to assure a frame structural response consistent with the joint rotational behaviour obtained from experimental tests and modelled as previously described, the values of column and beam material mechanical properties to be adopted in non-linear dynamic analyses are assumed equal to those measured in testing beam-to-column joint sub-assemblages and reported in Table 2. Regarding beam and column elements, a bilinear model characterized by a hysteretic behaviour with no stiffness degradation, no ductility-based strength decay, no hysteretic energy-based decay and no slip has been considered. However, it is useful to underline that this issue is not significant, because the use of partial-strength connections leads to the concentration of yielding in the connections, so that only the connection modelling is of primary importance.

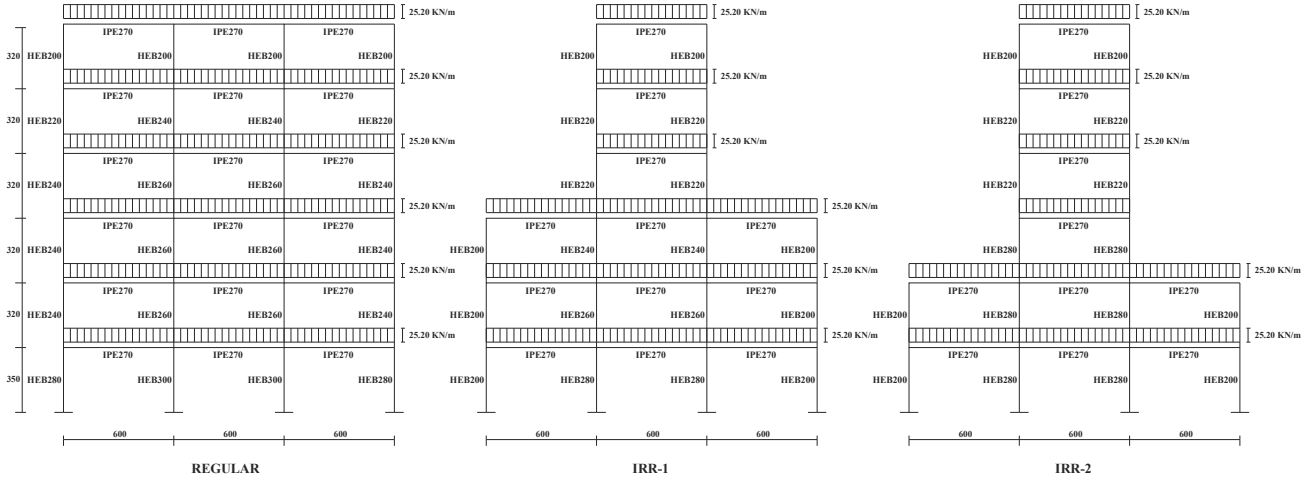

Figure 10. Analysed structural schemes

Table 2. Mechanical properties of members

	$f_{y,f}$ [N/mm^2]	$f_{u,f}$ [N/mm^2]	$f_{y,w}$ [N/mm^2]	$f_{u,w}$ [N/mm^2]
COLUMNS	430	523	382.5	522
BEAMS	405	546	387	534

4 INFLUENCE OF BEAM-TO-COLUMN JOINTS ON SEISMIC RESPONSE

The seismic performances of the examined MR-Frames with the four structural details of beam-to-column connections, previously described, have been investigated with the help of non-linear dynamic analyses, carried out by means of SeismoStruct computer program, for increasing levels of the seismic intensity measure. In particular, record-to-record variability is accounted for by performing Incremental Dynamic Analyses (IDA) considering 10 earthquake records selected from PEER database. Mass and stiffness proportional damping, 3% of critical value, has been assumed. The main data of the considered records (earthquake, component, date, peak ground acceleration, length, step recording) are reported in Table 3.

Aiming to perform IDA, all the records have been properly scaled to provide increasing values of the spectral acceleration Sa(T1) corresponding to the fundamental period of vibration of the structure. In the case of the regular frame, the period of vibration is equal to T_1=1.6 s for connections EEP-CYC 02 and EEP-DB-CYC 03 and equal to T_1=1.7 s for connections TS-CYC 04 and TS-M2-460-CYC-09. For the IRR-1, the period of vibration is equal to T_1=1.3 s for connections EEP-CYC 02, EEP-DB-CYC 03 and TS-M2-460-CYC-09 while for TS-M2-460-CYC-09 it is equal to 1.4 s. For the IRR-2 frame the period of vibration is equal to T_1=1.3 s for connections EEP-CYC 02 and EEP-DB-CYC 03 and equal to T_1=1.4 s for connections TS-CYC 04 and TS-M2-460-CYC-09. Scaling the records at the same value of Sa gives the possibility to reduce the variability of structural seismic response. In particular, the analyses have been repeated increasing the Sa(T1)/g value until the occurrence of connection collapse. Therefore, collapse has been identified by evaluating the spectral acceleration value leading to a maximum connection rotation equal to the ultimate value attained in the experimental tests. These values are delivered in Table 4 for EEP-CYC 02, EEP-DB-CYC 03 and TS-CYC 04 connections. Conversely, in the case of TS-M2-460-CYC-09 connection, reference

has been made to a limit value of the maximum drift (Table 4), because for such connection typology any desired rotation can be easily accommodated by properly designing the stroke of the friction dampers, i.e. the stroke of the slotted hole of the moving part of the T-stub stem. The target Maximum Interstorey Drift (MIDR) has been assumed as 0.10 according to FEMA [36] for the Near Collapse Limit State.

Table 3. Accelerogram characteristics

Earhquake (record)	Component	Date	PGA/g	Length (s)	Step recording (s)
Northridge (Stone Canyon)	SCR000	1994/01/17	0.252	39.99	0.01
Imperial Valley (Agrarias)	H-AGR003	1979/10/15	0.370	28.35	0.01
Kobe (Kakogawa)	KAK000	1995/01/16	0.251	40.95	0.01
Coalinga (Slack Canyon)	H-SCN045	1985/05/02	0.166	29.99	0.01
Victoria, Mexico (Chihuahua)	CHI102	1980/06/09	0.150	26.91	0.01
Spitak, Armenia (Gukasian)	GUK000	1988/12/17	0.199	19.89	0.01
Helena	A-HMC180	1935/10/31	0.150	39.99	0.01
Santa Barbara (Courthouse)	SBA132	1978/08/13	0.102	12.57	0.01
Friuli, Italy (Tolmezzo)	TMZ000	1976/05/06	0.351	36.35	0.005
Irpinia, Italy (Calitri)	A-CTR000	1980/11/23	0.132	35.79	0.0024

Table 4. Ultimate rotation of EEP-CYC 02, EEP-DB-CYC 03, TS-CYC 04 connections and ultimate interstorey drift for TS-M2-460-CYC 09 connections

	Ultimate Rotation (rad)
EEP-CYC 02	0.04
EEP-DB-CYC 03	0.06
TS-CYC 04	0.07
	Ultimate interstorey drift (rad)
TS-M2-460-CYC 09	0.10

With reference to the structural scheme “REGULAR”, figures 11 to 14 provide the IDA curves representing the maximum spring rotation for increasing values of the spectral acceleration. In particular, IDA analyses have been stopped for EEP-CYC 02, EEP-DB-CYC 03 and TS-CYC 04 connections when the first beam-to-column joint achieve the corresponding ultimate rotation as derived from experimental tests and reported in Table 4. Conversely, in case of connections equipped with friction dampers, i.e. TS-M2-460-CYC 09, for which the ultimate condition is assumed as the achievement of a MIDR equal to 0.10 the corresponding IDA curves (Fig. 14) have been stopped at a maximum spring rotation equal to 0.10. For this reason, in figures 15 to 18 the IDA curves providing the MIDR for increasing values of the spectral acceleration are also reported.

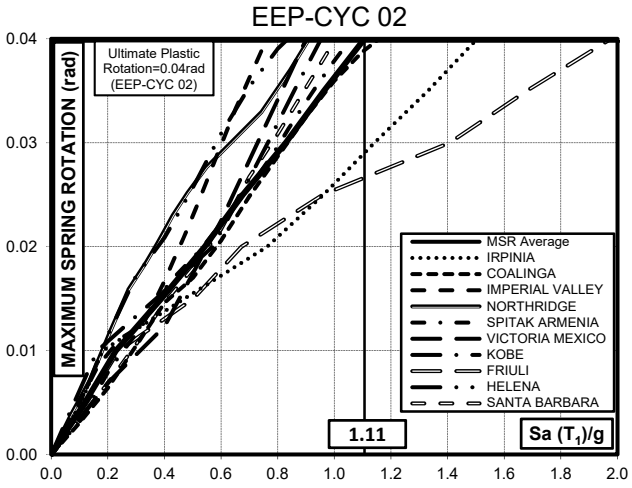

Figure 11. Maximum Spring Rotation vs Spectral Acceleration for EEP-CYC 02 connection for the regular MR-Frame

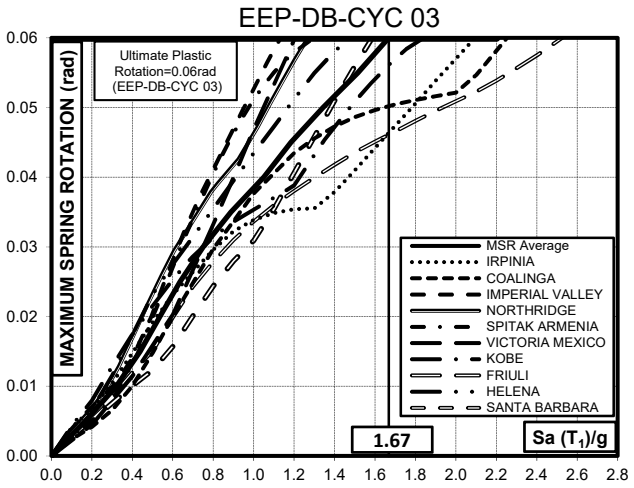

Figure 12. Maximum Spring Rotation vs Spectral Acceleration for EEP-DB-CYC 03 connection for the regular MR-Frame

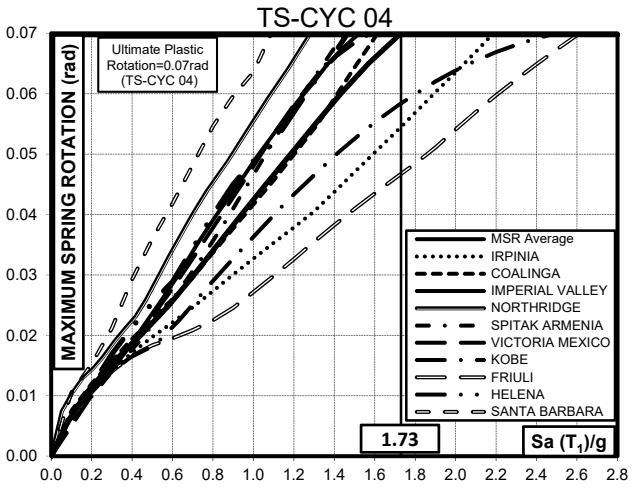

Figure 13. Maximum Spring Rotation vs Spectral Acceleration for TS-CYC 04 connection for the regular MR-Frame

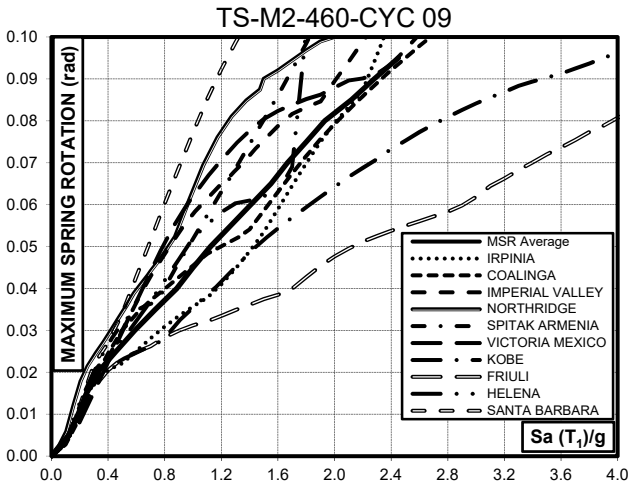

Figure 14. Maximum Spring Rotation vs Spectral Acceleration for TS-M2-460-CYC 09 connection for the regular MR-Frame

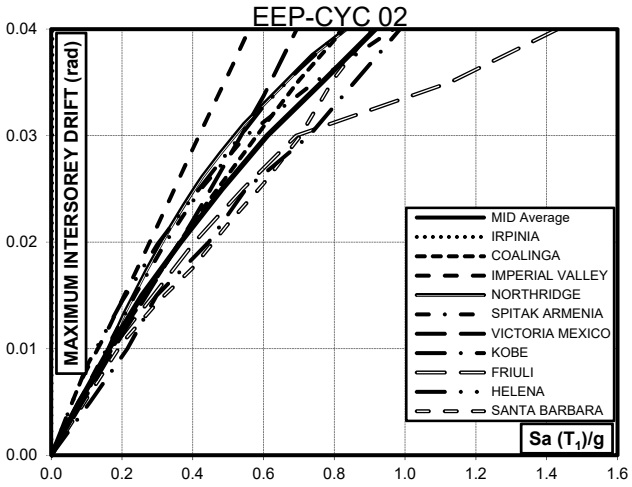

Figure 15. Maximum Interstorey Drift Ratio vs Spectral Acceleration for EEP-CYC02 connection for the regular MR-Frame

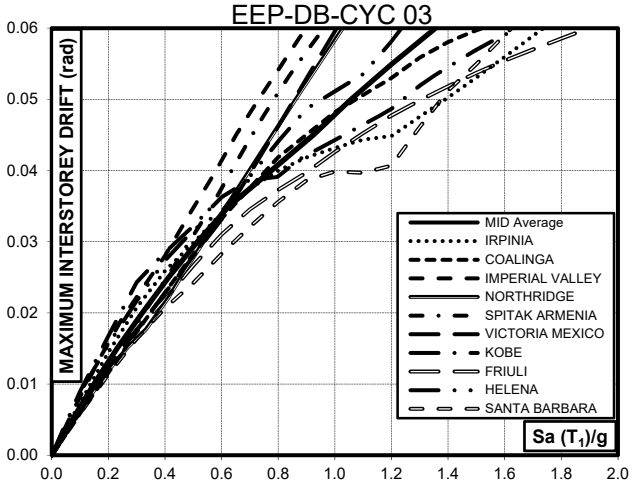

Figure 16. Maximum Interstorey Drift Ratio vs Spectral Acceleration for EEP-DB-CYC03 connection for the regular MR-Frame

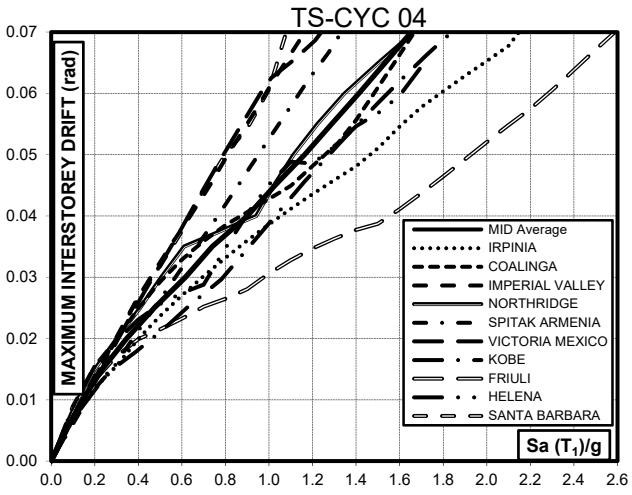

Figure 17. Maximum Interstorey Drift Ratio vs Spectral Acceleration for TS-CYC04 connection for the regular MR-Frame

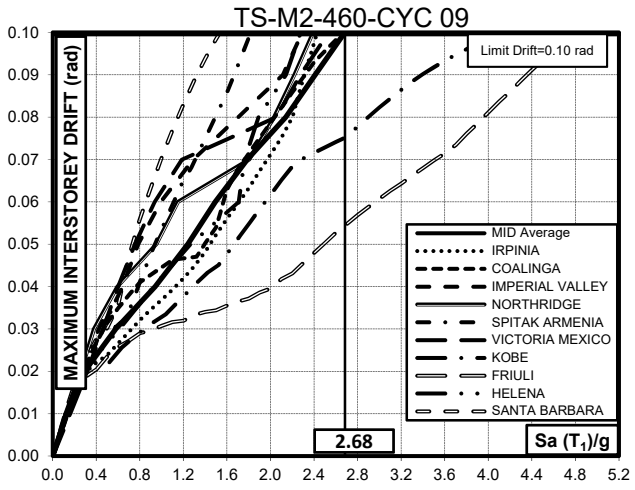

Figure 18. Maximum Interstorey Drift Ratio vs Spectral Acceleration for TS-M2-460-CYC 09 connection for the regular MR-Frame

The main result of the above analyses is the value of the spectral acceleration corresponding the attainment of the connection ultimate conditions assumed on the base of experimental evidence. Therefore, the seismic performances of the analysed structures in terms of ultimate spectral acceleration are reported in Table 5, where also the average value of the ultimate spectral acceleration for each connection typology is delivered.

Table 5. Spectral acceleration values corresponding to the achievement of the connections ultimate rotation for each considered earthquake record and with reference to the regular MR-frame

Earthquake	**EEP-CYC 02**	**EEP-DB-CYC 03**	**TS-CYC 04**	**TS-M2-460-CYC 09**
Coalinga	1.16	2.25	1.61	2.67
Imperial Valley	0.76	1.13	1.52	2.29
Northridge	0.91	1.27	1.29	2.39
Spitak Armenia	1.06	1.30	1.45	1.82
Victoria Mexico	0.90	1.20	1.58	2.53
Kobe	0.95	1.84	2.50	4.11
Friuli	1.98	2.53	2.61	4.78
Helena	0.84	1.48	1.47	2.28
Santa Barbara	1.00	1.59	1.09	1.54
Irpinia	1.50	2.09	2.19	2.43
Average $S_a(T_1)/g$	**1.11**	**1.67**	**1.73**	**2.68**

The same analyses have been carried out also with reference to the vertically irregular frames IRR-1 and IRR-2 which are characterized by the presence of set-backs. In particular, the maximum spring rotation vs spectral acceleration for the structural scheme IRR-1 and IRR-2 are reported in

Figures 19 to 22 and Figures 23 to 26, respectively. In addition, in Figure 27 to 30 and Figure 31 to 34 provide also the IDA curves in terms of MIDR vs spectral acceleration for the structural schemes IRR-1 and IRR-2, respectively.

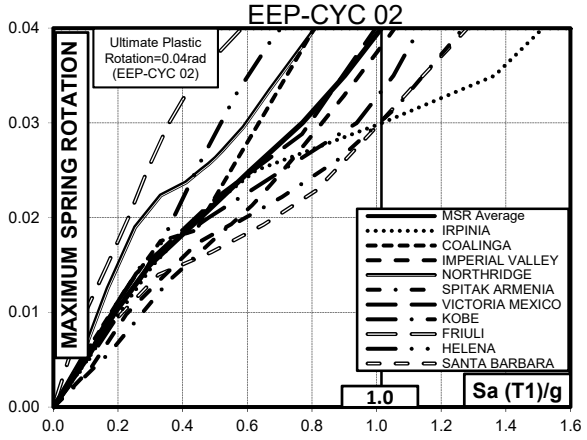

Figure 19. Maximum Spring Rotation vs Spectral Acceleration for EEP-CYC 02 connection and structural scheme IRR-1

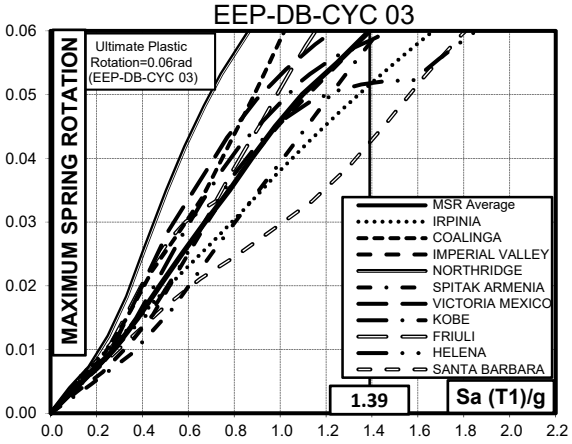

Figure 20. Maximum Spring Rotation vs Spectral Acceleration for EEP-CYC 03 connection and structural scheme IRR-1

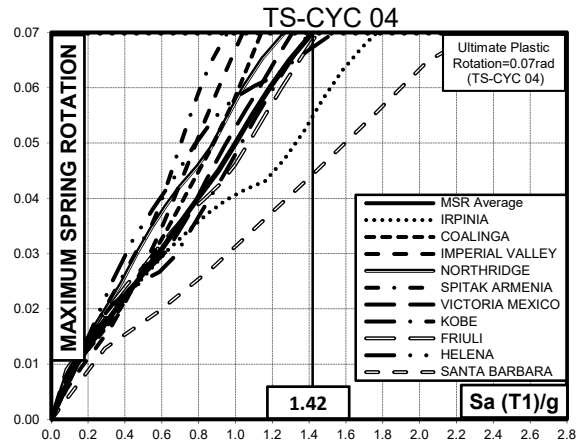

Figure 21. Maximum Spring Rotation vs Spectral Acceleration for TS-CYC 04 connection and structural scheme IRR-1

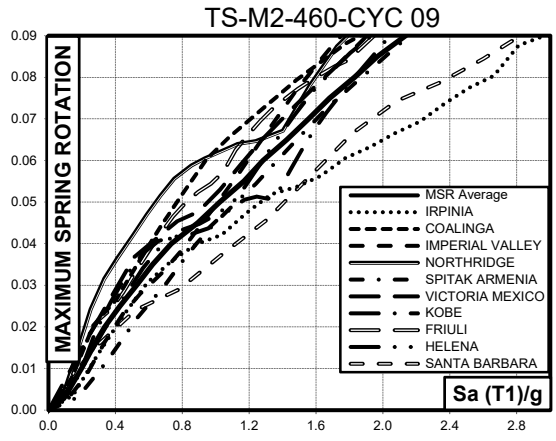

Figure 22. Maximum Spring Rotation vs Spectral Acceleration for TS-M2-460-CYC 09 connection and structural scheme IRR-1

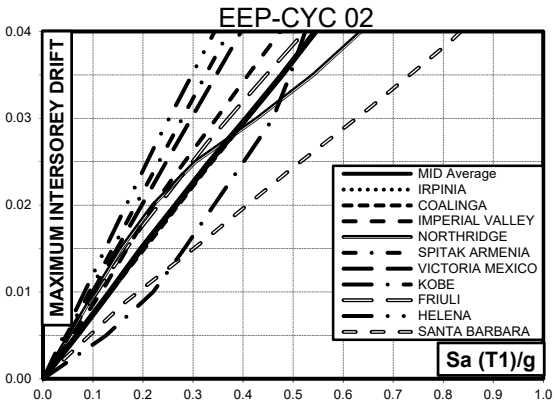

Figure 23. Maximum Interstorey Drift Ratio vs Spectral Acceleration for EEP-CYC02 connection and structural scheme IRR-1

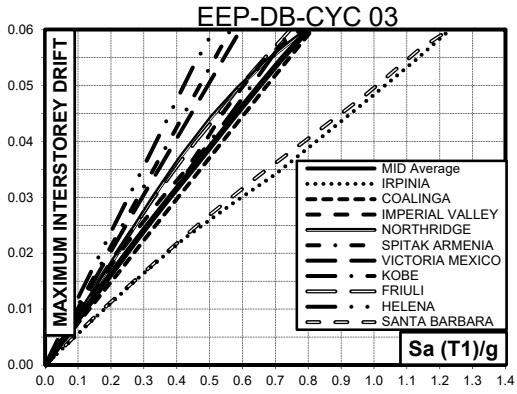

Figure 24. Maximum Interstorey Drift Ratio vs Spectral Acceleration for EEP-DB-CYC 03 connection and structural scheme IRR-1

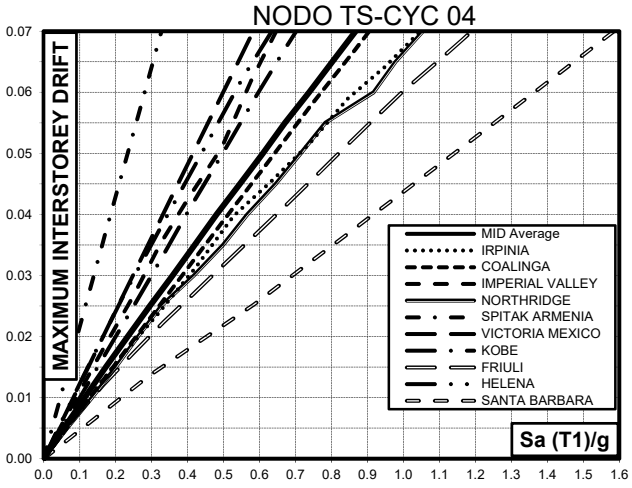

Figure 25. Maximum Interstorey Drift Ratio vs Spectral Acceleration for TS-CYC04 connection and structural scheme IRR-1

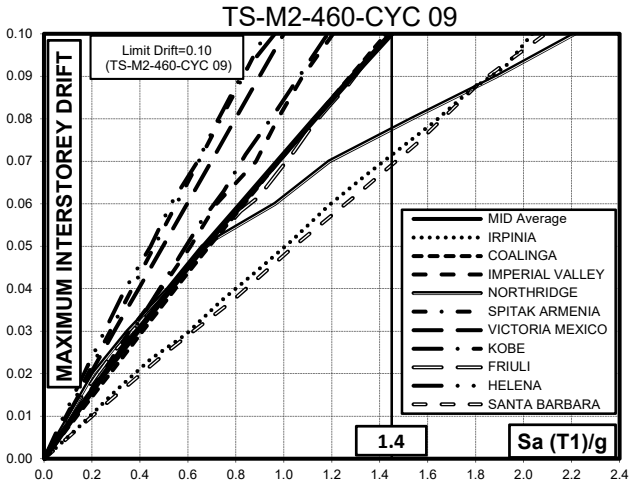

Figure 26. Maximum Interstorey Drift Ratio vs Spectral Acceleration for TS-M2-460-CYC 09 connection and structural scheme IRR-1

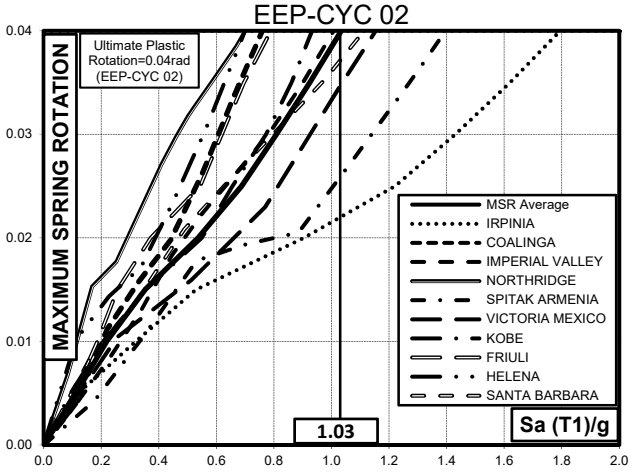

Figure 27. Maximum Spring Rotation vs Spectral Acceleration for EEP-CYC 02 connection and structural scheme IRR-2

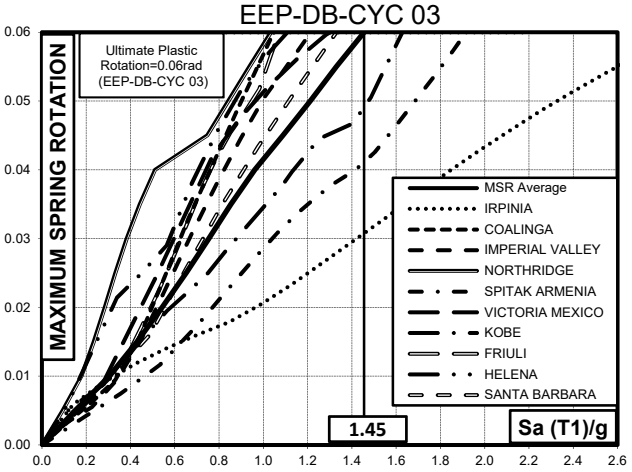

Figure 28. Maximum Spring Rotation vs Spectral Acceleration for EEP-DB-CYC 03 connection and structural scheme IRR-2

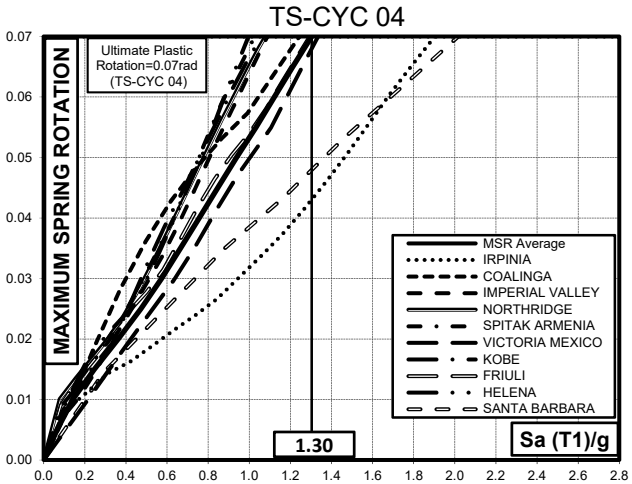

Figure 29. Maximum Spring Rotation vs Spectral Acceleration for TS-CYC 04 connection and structural scheme IRR-2

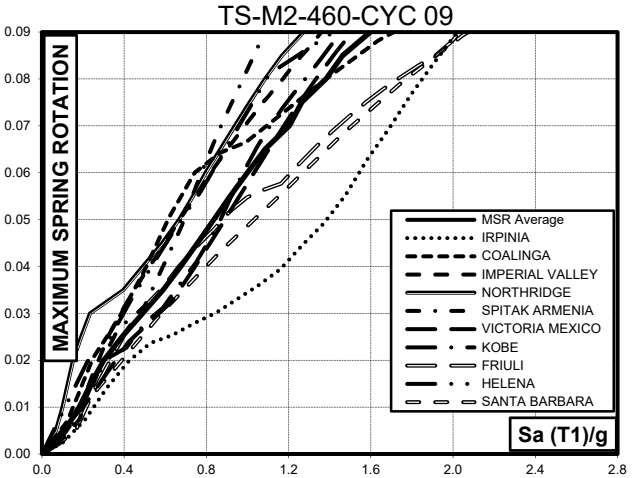

Figure 30. Maximum Spring Rotation vs Spectral Acceleration for TS-M2-460-CYC 09 connection and structural scheme IRR-2

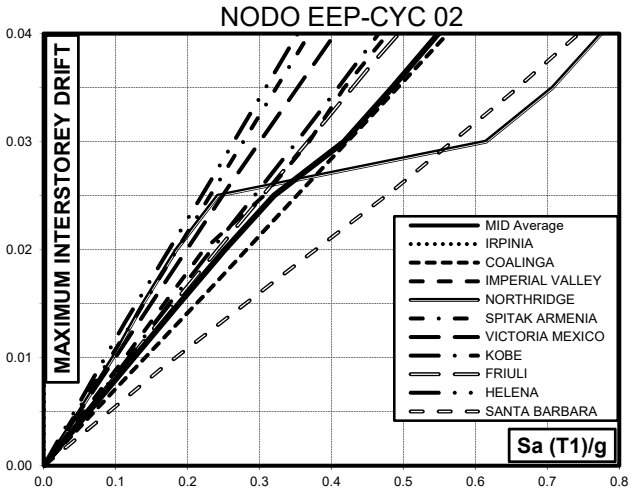

Figure 31. Maximum Interstorey Drift Ratio vs Spectral Acceleration for EEP-CYC02 connection and structural scheme IRR-2

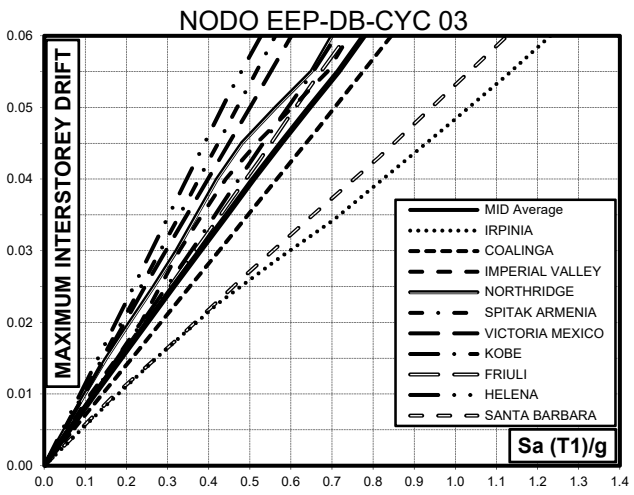

Figure 32. Maximum Interstorey Drift Ratio vs Spectral Acceleration for EEP-DB-CYC03 connection and structural scheme IRR-2

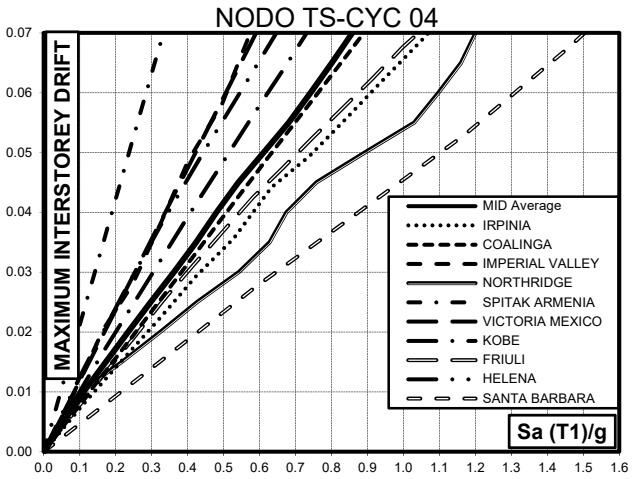

Figure 33. Maximum Interstorey Drift Ratio vs Spectral Acceleration for TS-CYC04 connection and structural scheme IRR-2

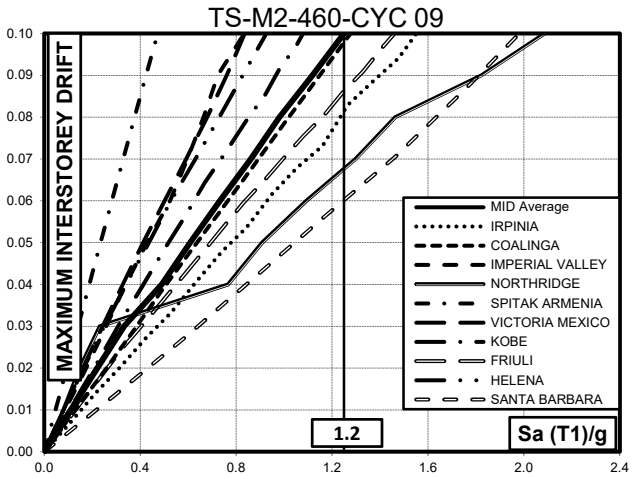

Figure 34. Maximum Interstorey Drift Ratio vs Spectral Acceleration for TS-M2-460-CYC 09 connection and structural scheme IRR-2

Table 6. Spectral acceleration corresponding to the achievement of the connections ultimate rotation for each considered earthquake record and with reference to structural scheme IRR-1

Earthquake	**EEP-CYC 02**	**EEP-DB-CYC 03**	**TS-CYC 04**	**TS-M2-460-CYC 09**
Coalinga	0.81	1.02	1.14	1.43
Imperial Valley	1.06	1.39	1.04	1.21
Northridge	0.81	0.87	1.27	2.21
Spitak Armenia	1.27	1.43	0.96	0.92
Victoria Mexico	1.00	1.23	1.31	1.00
Kobe	1.13	1.48	1.40	1.19
Friuli	0.58	1.15	1.45	1.44
Helena	0.70	1.85	1.54	0.96
Santa Barbara	1.28	1.81	2.32	2.09
Irpinia	1.51	1.67	1.77	2.04
Average $S_a(T_1)/g$	**1.02**	**1.39**	**1.42**	**1.45**

Table 7. Spectral acceleration corresponding to the achievement of the connections ultimate rotation for each considered earthquake record and with reference to structural scheme IRR-2

Earthquake	EEP-CYC 02	EEP-DB-CYC 03	TS-CYC 04	TS-M2-460-CYC 09
Coalinga	0.76	1.05	1.24	1.28
Imperial Valley	1.01	1.21	1.09	0.83
Northridge	0.70	1.03	1.08	2.09
Spitak Armenia	1.40	1.92	1.03	0.47
Victoria Mexico	1.15	1.30	1.33	0.84
Kobe	0.93	1.63	1.06	1.08
Friuli	0.79	1.07	1.29	1.46
Helena	0.70	1.11	1.00	0.93
Santa Barbara	1.11	1.33	2.02	1.98
Irpinia	1.79	2.90	1.90	1.55
Average $S_a(T_1)$/g	**1.03**	**1.45**	**1.30**	**1.25**

The values of the spectral acceleration leading to the attainment of the ultimate conditions are summarized in Table 6 and in Table 7 for the structural schemes IRR-1 and IRR-2, respectively.

The results of incremental dynamic non-linear analyses, delivered in the previous figures and tables, show the dependence on the record-to-record variability. Therefore, in order to point out, on one hand, the main effects of the connection typology and, on the other hand, the influence of the structural scheme, they are further summarized in Table 8 where reference is made to the average value of the spectral acceleration leading to the attainment of the ultimate conditions.

Table 8. Values of the average spectral acceleration corresponding to the achievement of the ultimate conditions

	$S_a(T_1)$/g		
	REGULAR	IRR-1	IRR-2
EEP-CYC 02	1.11	1.02	1.03
EEP-DB-CYC 03	1.67	1.39	1.45
TS-CYC 04	1.73	1.42	1.30
TS-M2-460-CYC 09	2.68	1.45	1.25

First of all, it is important to underline that the examined partial-strength connections have been designed to attain the same degree of flexural resistance with respect to the connected beam. In addition, also the rotational stiffness is very similar as testified by the period of vibration which, as an example, with reference to the regular frame is equal to 1.6 sec for connections EEP-CYC02 and EEP-DB-CYC03 and equal to 1.7 sec for connections TS-CYC04 and TS-M2-460-CYC-09. Therefore, the influence of the connection typology is practically due, on one hand, to the

corresponding available rotation capacity and, on the other hand, to the quality and stability of the hysteresis loops.

In particular, frames with partial strength extended end-plate connections (EEP-CYC02) show the worst performances for all the selected earthquake records and for all the investigated structural schemes, because they provide the minimum rotation capacity equal to 0.04 rad. As testified by the experimental test [27], as the displacement amplitude increases the plastic engagement of the end-plate at the welded connection between the beam flange and the end-plate increases. In the case of the tested specimen, this has led to the formation and progressive development of a crack along the whole width of the end-plate starting from the middle of the heat affected zone. This crack progressively propagated up to the complete fracture of the end-plate. The end-plate in bending was designed to assure a type-1 mechanism according to Eurocode 3 and, therefore, the failure mode obtained from the experimental test is consistent with the design criterion, but, because of the heat affected zone it has provided a reduction of the plastic rotation supply under cyclic loads.

Regarding the RBS connection (EEP-DB-CYC03), the bolted T-stub connection (TS-CYC04) and the double split tee connection equipped with friction dampers (TS-M2-460-CYC09), all of them have exhibited better seismic performances if compared with EEP-CYC02. However, it is not possible to give a quick answer on what is the typology leading to the best structural performances. In fact, RBS connections (EEP-DB-CYC03) leads, on average, to the best seismic performance only in the case of structural scheme IRR-2 followed by T-stub connections (TS-CYC04) and connections equipped with friction dampers (TS-M2-460-CYC09) while in the case of the regular MR-Frame and in the case of the structural scheme IRR-1 the connection equipped with friction dampers exhibit, on average, the best performances compared to the other connection typologies.

This results are justified by the connection characteristics in term of ductility, hysteresis loops and ultimate deformation capacity. In fact, with reference to traditional connections, the bolted T-stub connection (TS-CYC04) assures the highest plastic rotation supply, equal to 0.07 rad (Table 4) which is able to redeem the significant pinching effects. Conversely, RBS connection (EEP-DB-CYC03) exhibit a lower plastic rotation supply (0.06 rad, Table 4) compared to TS-CYC04 connection, but more stable hysteresis loops that lead in some cases to seismic performances similar those achieved by means of T-stub connections. The use of connections equipped with friction dampers (TS-M2-460-CYC09) deserves a separate discussion, because the ultimate performances are governed, in this case, by the assumed value of ultimate drift. In fact, the rotation supply of the connection can be easily designed in order to accommodate the expected rotation demand. This can be properly obtained by increasing the length of slotted holes which define the end-stroke of the friction damper. In addition, it is important to observe that also after the achievement of the

maximum device stroke, i.e. after the attainment of the end-stroke limit state, collapse does not occur, because of the activation of new resistant mechanism which is characterize by the engagement of the bolts of the friction devices in shear resistance and of the corresponding plates in bearing. Therefore, the use of connections equipped with friction dampers is even more promising than table 8 points out.

Regarding the influence of the vertical geometrical irregularity, it has to be preliminarily underlined that all the structural scheme have been designed to assure a collapse mechanism of global type by means of the theory of plastic mechanism control. The use of a design approach assuring the same collapse mechanism typology allow to focus on the effects of vertical geometrical irregularity only.

To this aim, for any given connection typology, the results obtained have to be compared considering the different structural schemes examined. In particular, the results show that MR-Frames with "set-backs" are generally subjected to a ductility demand greater than those required to the regular MR-Frames. In fact, the regular MR-Frames show better seismic performances when compared to the irregular structures. This is testified by the ratios reported in Table 9 which point out that seismic performances of irregular MR-Frames are about 20-25% less than those exhibited by the starting regular frame. This result seems in line with the recommendation provided by Eurocode 8 [2] which suggests a 20% reduction of the behaviour factor in case of vertically irregular structures.

Table 9. Ratios between the collapse value achieved by irregular frame and those provided by the regular one

	$S_{a,C,Irr-1}/ S_{a,C,Reg}$	$S_{a,C,Irr-2}/ S_{a,C,Reg}$
EEP-CYC 02	0.92	0.93
EEP-DB-CYC 03	0.83	0.87
TS-CYC 04	0.82	0.75
TS-M2-460-CYC 09	0.54	0.47
Average	**0.78**	**0.75**

5 CONCLUSIONS

Nowadays semi-rigid partial-strength connections, if well designed, can be considered to have sufficient ductility and dissipation capacity in order to satisfy the seismic demand. Therefore, in this paper the influence of beam-to-column connections on the seismic response of MR-Frames has been studied by investigating both a regular MR-Frame and two vertically irregular MR-Frames with "set-backs".

Starting from the knowledge of the cyclic rotational behaviour of beam-to-column joints, four different structural details of beam-to-column connections have been considered. In particular, three traditional connection typologies, extended end-plate, RBS and bolted T-stub connections, and one innovative typology,

T-stub connection equipped with friction dampers, have been examined. Incremental dynamic non-linear analyses have been carried out by means of SeismoStruct computer program and modelling the cyclic behaviour of the connections by means of its smooth hysteretic model, whose parameters have been calibrated on the base of available experimental tests, obtaining a good agreement between experimental and modelled behaviour.

Concerning the influence of the connections typology, the results show that extended end-plate connections (namely EEP-CYC 02) always exhibited the worst performances. In particular, in the case of the regular frame and in the case of structural scheme IRR-1 the connection providing the best seismic performances is, on average, that equipped with friction dampers (TS-M2-460-CYC09), while, in the case of structural scheme, RBS connections exhibited, on average, the best seismic performances. However, the bolted T-stub connection equipped with friction pads is the most suitable to accommodate higher interstorey drifts, because the stroke of the devices can be properly increased by modifying the length of the slotted holes of the moving component of the friction damper.

Regarding the comparison in terms of seismic performances between the regular frame and those with "set-backs", it has been observed that the schemes with set-backs providing a vertical irregularity lead, on average, to a 20-25% reduction of the ultimate value of the spectral acceleration when compared with the starting regular frame. This confirms the 20% reduction of the behaviour factor proposed by commonly used seismic rules. Therefore, it can be concluded that semi-rigid partial-strength connections, if well designed, are able to assure sufficient ductility to satisfy the seismic demand not only for regular MR-Frames but even in the case of irregular MR-Frames with "set-backs".

6 REFERENCES

[1] ANSI-AISC 341-10 (2010). Seismic Provisions for Structural Steel Buildings, American Institute of Steel Construction, Chicago, Illinois.

[2] CEN (2005). EN 1998-1-1: Eurocode 8 - Design of Structures for Earthquake Resistance. Part 1: General Rules, Seismic Actions and Rules for Buildings. CEN/TC 250.

[3] Mazzolani F.M., Piluso V. (1997): "Plastic design of seismic resistant steel frames", Earthquake Engineering and Structural Dynamics, vol. 26, pp. 167-191.

[4] Mazzolani, F. M. and Piluso, V. (1996). Theory and Design of Seismic Resistant Steel Frames, E & FN Spon, London.

[5] Bruneau, M., Uang, C. M., and Whittaker, A. (1998). Ductile Design of Steel Structures, McGraw Hill, New York.

[6] Faella, C., Piluso, V. and Rizzano, G. (2000). Structural Steel Semirigid Connections, CRC Press, Boca Raton, Florida.

[7] Moore, K.S., Malley, J. O., and Engelhardt, M. D. (1999). Design of Reduced Beam Section (RBS) Moment Frame Connections, AISC Structural Steel Educational Council, Moraga, CA.

[8] Montuori, R., Piluso, V. (2000). Plastic Design of Steel Frames with Dog-Bone Beam to Column Joints.

STESSA 2000, Behaviour of steel structures in seismic areas, Montreal, Canada 21-24 August 2000 Rotterdam Balkema Vol.1, Pag.208-215

[9] FEMA 351 (2000). Recommended seismic evaluation and upgrade criteria for existing welded steel moment-frame buildings, Federal Emergency Management Agency, Washington, D.C.

[10] Montuori, R. (2015). The Influence of Gravity Loads on the Seismic Design of RBS Connections. Open Construction and Building Technology Journal, January 2015 Pages 248-261 DOI: 10.2174/1874836801408010 24.

[11] Montuori R. (2015). Design of "Dog-Bone" Connection: The Role of Vertical Loads - COMPDYN 2015 Thematic Conference on Computational Methods in Structural Dynamics and Earthquake Engineering - Crete Island, Greece, 25–27 May 2015.

[12] Faella, C., Piluso, V., and Rizzano, G. (1997). A new method to design extended end plate connection and semirigid braced frames, Journal of Constructional Steel Research 41(1), 61-91.

[13] Faella, C., Montuori, R., Piluso, V., and Rizzano, G. (1998). Failure mode control: economy of semi-rigid frames, Proc. of the XI European Conference on Earthquake Engineering, Paris.

[14] Khoo, H-H., Clifton, G., Butterworth, J., MacRae, G. (2012). Developments on the Sliding Hinge Joint. 15th World Conference on Earthquake Engineering. Lisboa 2012, paper n. 1766.

[15] Khoo, H-H., Clifton, G., Butterworth, J., MacRae, G., Gledhill, S., Sidwell, G. (2012). Development of the self-centering Sliding Hinge Joint with friction ring springs. Journal of Constructional Steel Research 78 (2012) 201–211.

[16] Khoo, H-H., Clifton, G., Butterworth, J., MacRae, G., Ferguson, G. (2012). Influence of steel shim hardness on the Sliding Hinge Joint performance. Journal of Constructional Steel Research 72 (2012) 119–129

[17] Butterworth, J., Clifton, G., (2000). Performance of Hierarchical Friction Dissipating Joints in Moment Resisting Steel Frames. 12th World Conference on Earthquake Engineering. Paper n. 718.

[18] Khoo H-H., Clifton, C., MacRae, G., Zhou, H., Ramhormozian, S. (2014). Proposed design models for the asymmetric friction connection. Earthquake Engineering & Structural Dynamics, DOI: 10.1002/eqe.2520.

[19] Latour M., Rizzano G., Piluso V. (2015). Free from damage beam-to-column joints: Testing and design of DST connections with friction pads. Engineering Structures 85, 219-233.

[20] Jaspart, J. P. (1991). Etude de la semi-rigide des noeuds Poutre-Colonne et son influence sur la resistence et la stabilite des ossature en acier, PhD Thesis, University of Liege, Belgium.

[21] CEN (2005). EN 1993-1-1:2005. Eurocode 3: Design of steel structures. Part 1: General rules and rules for buildings. CEN/TC 250.

[22] Faella, C., Piluso, V., and Rizzano, G. (1998). Cyclic Behavior of bolted joints components, Journal of Constructional Steel Research 46 (1-3), paper 129.

[23] Kim, K.D. and Engelhardt, M.D. (2002). Monotonic and Cyclic Loading Models for Steel Panel Zones in Steel Moment Frames, Journal of Constructional Steel Research, Vol. 58, pp. 605-635.

[24] Clemente, I, Noè, S. and Rassati, G.A. (2004). Experimental Behaviour of T-stub Connection Components for the Mechanical Modelling of Bare Steel and Composite Partially Restrained Beam-to-Column Connections, International Workshop on Connections in Steel Structures, Amsterdam, June 3-4, 2004.

[25] Dubina, D., Stratan, A., Muntean, N., Grecea, D. (2008). Dual steel T-stub behaviour under monotonic and cyclic loading, International Workshop on Connections in Steel Structures, Chicago, June 25, 2008.

[26] Hu, J.W., Leon, R.T. and Park, T. (2011). Mechanical Modeling of Bolted T-stub Connections under Cyclic Loads. Part I: Stiffness Modeling, Journal of Constructional Steel Research, Vol. 67, Issue 11, pp. 1710-1718.

[27] Iannone, F., Latour, M., Piluso, V. and Rizzano G. (2011). Experimental Analysis of Bolted Steel Beam-to-Column Connections: Component Identification, Journal of Earthquake Engineering 15, 215-244.

[28] Latour, M., Piluso, V. and Rizzano G. (2011). Cyclic Modelling of Bolted Beam-to-Column Connections: Component Approach, Journal of Earthquake Engineering, Vol. Volume 15, Issue 4, pp.537- 563, 2011.

[29] Latour M., Rizzano G., Piluso V. (2012): "Experimental Analysis of Innovative Dissipative Bolted Double Split Tee Beam-to-Column Connections", Steel Construction, 4 (2011), N.2, pp. 53-64.

[30] Latour M., Rizzano G., Piluso V. (2013): "Experimental behaviour of friction T-stub beam-to-column joints under cyclic loads", Steel Construction, 6, No. 1, p.11-18.

[31] Piluso V., Faella C., Rizzano G. (2001). Ultimate Behaviour of bolted T-stubs, I: theoretical model. Journal of Structural Engineering, ASCE, 127(6), 686-693, 2001.

[32] Montuori, R., Piluso, V., Troisi, M. (2012). Influence of Connection Typology on the Sesimic Behaviour of MR-Frames. Connections VII, 7th International Workshop on Connections in Steel Structures, Timisoara, Romania, May 30 – June 2, 2012, pp. 133-146, ISBN: 978-92-9147-114-0.

[33] Rizzano, G. [2006]. Seismic Design of Steel Frames with Partial Strength Joints, Journal of Earthquake Engineering, 10 (5), 725-747.

[34] Piluso V., Nastri E., Montuori R., "Advances in Theory of Plastic Mechanism Control: Closed Form Solution for MR-Frames", Earthquake Engineering and Structural Dynamics, 2014

[35] R. Montuori, V. Piluso, M. Troisi: "Theory of Plastic Mechanism Control of Seismic Resistant MR-Frames with Set-Backs", The Open Construction and Building Technology Journal, Volume 6, 2012, pp. 404-413, 2012.

[36] FEMA 355F, "State of the Art Report on Performance Prediction and Evaluation of Steel Moment-Frame Buildings", Federal Emergency and Management Agency, September 2000.